IJE TRANSACTIONS B: Applications Vol. 37 No. 08, (August 2024) 1510-1521

International Journal of Engineering

Journal Homepage: www.ije.ir

Performance Evaluation of Artificial Neural Networks and Support Vector Regression in Tunneling-Induced Settlement Prediction Incorporating Umbrella Arch Method Characteristics

M. Arjmandazar Varjovi[a], M. Rahmanpour[a], M. H. Khosravi*[b], A. Majdi[a], B. T. Le[c]

[a] *School of Mining Engineering, College of Engineering, University of Tehran, Tehran, Iran*
[b] *Department of Mining Engineering, Faculty of Engineering, University of Birjand, Birjand, Iran*
[c] *Faculty of Science and Engineering, Anglia Ruskin University, Chelmsford, United Kingdom*

PAPER INFO

Paper history:
Received 10 November 2017
Received in revised form 23 December 2017
Accepted 04 January 2018

Keywords:
Surface Settlement
Settlement Prediction
Umbrella Arch Method
Artificial Neural Networks
Support Vector Regression

ABSTRACT

Accurate settlement forecasting is essential for preventing severe structural and infrastructure damage. This paper investigates predicting tunneling-induced ground settlements using machine learning models. Empirical methods for estimating settlements are often imprecise and site-specific. Developing novel, accurate prediction methods is critical to avoid catastrophic damage. The umbrella arch method constrains deformations for initial stability before installing primary support. This study develops machine learning models to forecast settlements solely from umbrella arch parameters, disregarding soil properties. Multilayer perceptron artificial neural networks (MLP-ANN) and support vector regression (SVR) are applied. Results demonstrate machine learning outperforms empirical methods. The MLP-ANN surpasses SVR, with R^2 of 0.98 and 0.92, respectively. Strong correlation is observed between umbrella arch configuration and settlements. The suggested approach effectively estimates surface displacements lacking mechanical properties. Overall, this study supports machine learning, specifically MLP-ANN, as an efficient, reliable alternative to empirical methods for predicting tunneling-induced ground settlements from umbrella arch design.

***doi**: 10.5829/ije.2024.37.08b.05*

Graphical Abstract

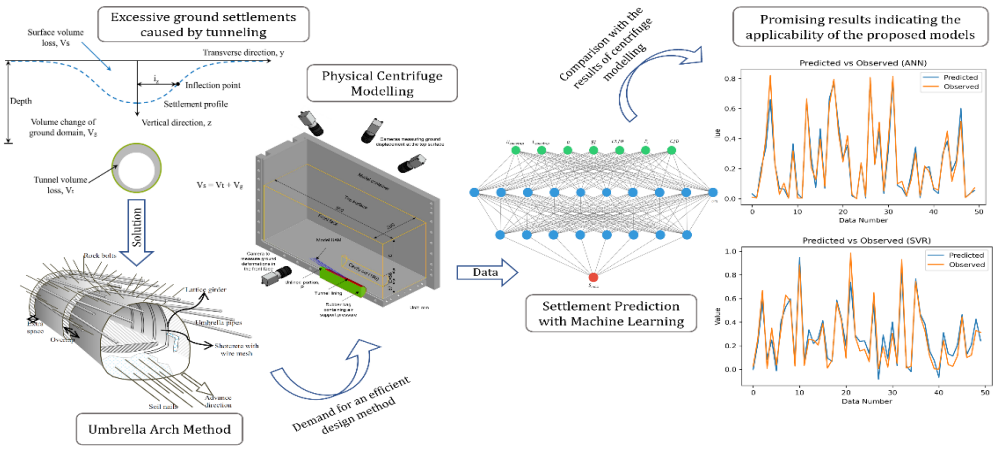

*Corresponding Author Email: mh.khosravi@birjand.ac.ir (M. H. Khosravi)

Please cite this article as: Arjmandazar Varjovi M, Rahmanpour M, Khosravi MH, Majdi A, Le BT, Performance Evaluation of Artificial Neural Networks and Support Vector Regression in Tunneling-Induced Settlement Prediction Incorporating Umbrella Arch Method Characteristics. International Journal of Engineering, Transactions B: Applications. 2024;37(08):1510-21.

NOMENCLATURE

V_t	Tunnel volume loss (m^3)	EI	Pipe flexural rigidity
V_s	Surface volume loss (m^3)	EL	Forepole embedded length
$S_{z,y}$	Settlement at a distance of y and a depth of z_0 from the surface (mm)	P_s	Tunnel face support pressure
S_{max}	Maximum ground surface settlement (mm)	K	Feature vector of RBF kernel
i_z	Horizontal distance from the tunnel centerline to the inflection point of the settlement trough (m)	R_{xy}	Pearson's correlation coefficient between x and y
C	Tunnel cover depth (m)	**Greek Symbols**	
D	Tunnel diameter (m)	α	Symmetric crown coverage angle of the forepoles (degrees)
$U_{spacing}$	Spacing between crown forepoles	ξ_i	Slack variable of the i-th observation
$L_{spacing}$	Spacing between shoulder forepoles	ε	Epsilon-tube margin

1. INTRODUCTION

Sustainable development in urban areas has substantially increased the demand for underground openings. Among them, tunnels are of great importance since they are constructed to facilitate transportation, sewerage disposal, etc. The construction of these facilities is intrinsically complex and inevitably induce ground settlements due to the tunnel convergence and redistribution of in-situ stresses (1, 2). During the tunneling excavation process, the volume of soil that is being excavated is inevitably greater than the volume of soil that represents the theoretical volume of the tunnel. This over-excavated volume is considered as tunnel volume loss (V_t). Moreover, the factors like creep, consolidation and, hydraulic fluctuations can increase the volume loss (3). The surface volume loss (V_s) is a measure that describes the disturbance of the overall state of the ground caused by tunnel excavation. It causes a Gaussian settlement curve on the ground as follows:

$$S_{z,y} = S_{max} \exp\left(\frac{-y^2}{2i_z^2}\right) \quad (1)$$

where, $S_{z,y}$ is the settlement at a transverse distance of y and a depth of z from the surface (Figure 1a); i_z is the horizontal distance from the tunnel centerline to the inflection point of the settlement trough (Figure 1b); and S_{max} is the maximum ground surface settlement. The geometry of the tunneling-induced settlements profile is illustrated in Figure 1. Under undrained conditions, the volume of the settlement trough is equal to the tunnel volume loss. According to Peck, the i_z value of transverse tunneling-induced settlement profile can be obtained through the following equation:

$$\frac{i_z}{R} = \left(\frac{z_o}{2R}\right)^n \quad ,n = 0.1 \text{ to } 0.8 \quad (2)$$

where, z_0 is the tunnel axis depth and R is the tunnel radius. V_s is mathematically expressed as the ratio of the difference between the excavated soil volume and the theoretical volume of the tunnel to the practical volume of the tunnel. The volume loss per unit meter of the tunnel length is defined as settlement curve integration as follows (4):

$$V_s = \int S_{z,y}.dy = S_{max} \exp\left(\frac{-y^2}{2i_z^2.dy}\right) = S_{max}\sqrt{2\pi}i_z \quad (3)$$

In general, excavation-induced ground settlements are predicted through different empirical and numerical approaches that comprise a variety of factors including geological conditions, tunnel depth and geometry of the premiere as well as excavation method, etc. (5, 6). Excessive ground surface settlement may lead to considerable damage to nearby structures (7, 8). Hence, precautionary considerations should be taken to minimize the settlement. The Umbrella Arch Method (UAM), also known as Umbrella Pipe Arch or Forepoling Umbrella System, is considered as an effective measure for improving the operational safety as well as mitigating the tunneling-induced ground settlements and thus, preventing the structural damage to adjacent facilities (1-5, 9-11). Due to its capabilities in yielding the stress distribution in small scale analogous to a full scale prototype, centrifuge modelling has been widely used for studying excavation-induced geotechnical problems (12, 13). Numerous researchers have investigated the application of geotechnical centrifuge in exploring tunneling induced three-dimensional ground settlements (12, 14-21). Lu et al. (21)conducted centrifuge modeling to investigate the influence of forepole insertion angles and cover-to-tunnel diameter ratios on ground settlement. Their results indicate that the major influenced zone along the longitudinal direction is ±1.25D, where D is the tunnel diameter (21). Juneja et al. (14) investigated the effects of forepoles and unsupported length on tunnel face stability through 100g centrifuge modelling. They suggested that the tunnel stability depends not only on the unsupported length of the tunnel but also on the length of forepoles (14).

In order to represent the effects of UAM shell on settlement, Divall et al. (16) used stiff resin inclusions

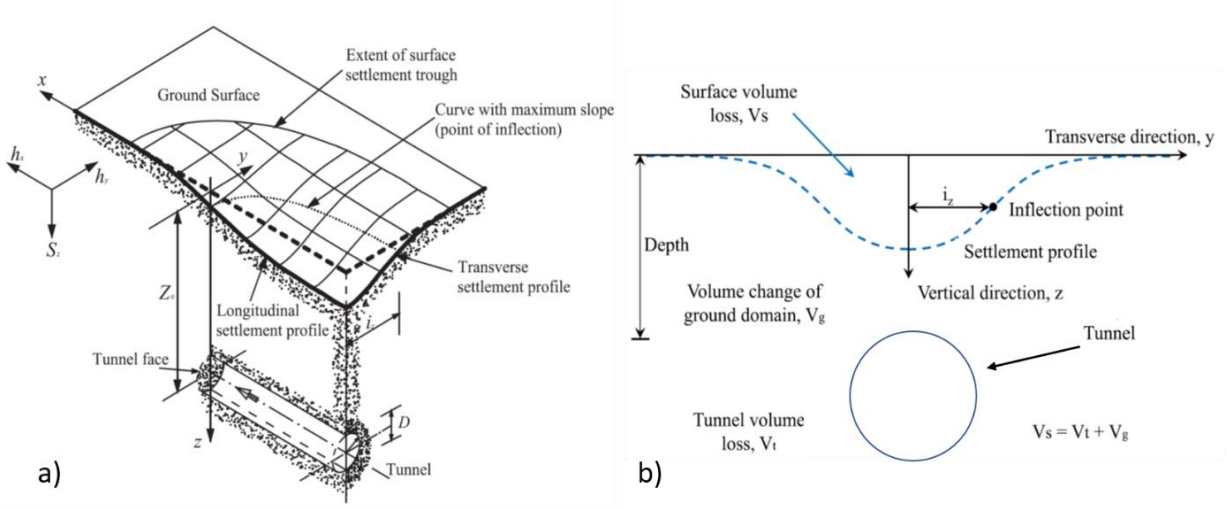

Figure 1. Geometry of the tunneling-induced settlement trough in: (a) 3D perspective (10), (b) Transverse settlement profile (after (11))

around the annulus of a single tunnel. They monitored the deformation zone around the tunnel via image processing and displacement transducers. The results of their study indicated the influence of forepoling layout on plastic collapse mechanism (16). Le and Taylor (20) concluded similar modelling, emphasizing on forepoling pipe characteristics and arrangement. Owing to the potential of tackling the uncertainties and inaccuracies associated with almost every engineering project, soft computing methods were developed to provide data-driven approaches for complex engineering problems with robust and precise solutions (22).

In recent years, soft computing techniques were successfully applied in geomechanics and particularly, in tunneling (23-26). The use of soft computing in tunneling has led to an enhanced understanding of operational conditions and the identification of probable parametric correlations (27). Machine learning (ML) algorithms have been widely used in estimating tunneling-induced ground settlements where the empirical methods fail to precisely anticipate the ground deformations (28-31). Ahangari et al. (30) studied the application of Gene Expression Programming (GEP) and Adaptive Neuro-Fuzzy Inference System (ANFIS) in predicting subway settlements for a case study of 53 tunnels excavated with the NATM method. Their models included a combination of soil strength properties (i.e., angle of internal friction, cohesion, and Young's modulus), tunnel depth and diameter. The corresponding settlement which was obtained through numerical analysis. The results indicated that both models possessed a considerably high accuracy in mapping deformations. They have acknowledged that the intelligent approaches are excellent tools for handling problems with complicated systems and various affecting elements like excavation-induced settlement prediction since there are no restrictions on the number of input parameters that can be used to forecast geotechnical parameters with these approaches (30). Zhang et al. (28) proposed a unique hybrid approach that combined wavelet packet transformation (WPT) and least-squares support vector machines (LSSVMs) to develop a model with improved capability for estimating the surface displacements caused by tunnel excavation. In this context, they have considered the Wuhan metro, China as a case study to prove the operational feasibility of the WPT-LSSVM model. The results suggested that the intelligent models outperform the available analytical methods in terms of accuracy. Furthermore, they stated that the WPT-LSSVM provides higher accuracy and dependability than the classic LSSVM approach in calculating tunnel-induced settlement. They have also concluded that the developed method can be used as a decision-making technique for time-series analysis and calculation of tunnel-induced displacements, which can help to improve project safety (28).

Criticizing the limited and time-consuming nature of the empirical methods, Moghaddasi and Noorian-Bidgoli (32) provided a predictive model based on an artificial neural network optimized with the Imperialist competitive algorithm (ICA) for predicting the maximum surface settlement. They obtained a dataset comprising the lateral stress ratio, the modulus of elasticity, cohesion, and their corresponding maximum settlement that occurred on the ground surface from a case study tunnel in Karaj subway, Iran. The results demonstrated the significant efficiency of the trained models with 0.9806 and 0.9402 R^2 scores for the ICA-ANN and ANN models, respectively. Since the developed models relied on the mechanical properties of the ground in the Karaj

subway, they suggested the researchers to modify their models with respect to the geological conditions inherent to the tunnel project being studied. In addition, they have encouraged the researchers to incorporate further input parameters including tunnel operational parameters in developing settlement prediction models (32). In order to estimate ground settlement during shield tunneling, Zhang et al. (33) suggested using artificial intelligence to take into account interactions among several aspects, such as geological formations, construction variables, construction phases, and grout properties. Their methodology employed a hybrid ANN model that integrated an artificial neural network with a differential evolutionary (DE) optimization algorithm (ANN-DE). The optimum architecture and ANN hyperparameters were chosen using the DE technique. Their suggested hybrid model was utilized for settlement prediction in a real-world scenario involving mechanized tunneling in Guangzhou subway, China. The findings of the sensitivity analysis showed that the three key operational factors influencing settlement at the surface were face pressure, excavation deviation, and shield thrust. They also addressed that their proposed hybrid intelligent model with a R^2 score of 0.9123 can be a good alternative to the empirical methods (33). However, their model cannot be applied to real-time engineering practices due to insufficient accuracy, which is valid not only in the field of underground and tunnel construction but also in many other engineering projects. It is necessary to find models of natural variables with a higher degree of adequacy (34).

The aforementioned researches were engaged with the application of machine learning algorithms in predicting the ground displacements caused by tunneling based on soil properties and operational parameters. The aftermath of these researches proved the superiority of the machine learning algorithms over empirical methods. Nevertheless, the influence of UAM design parameters on settlement prediction has not been investigated yet. The aim of this study is to evaluate the performance of artificial neural networks and support vector regression in tunneling-induced ground settlement prediction incorporating the UAM characteristics. In order to maintain the independence of the proposed models against the site-specific soil mechanical properties and make an all-inclusive deduction of the UAM effects on controlling the settlements, the mechanical properties of the soil were excluded in the modeling procedure.

1. 1. The Theoretical Background of the Umbrella Arch Method of Reinforcement In UAM, in order to maintain tunnel heading stability, the longitudinal pipes are installed through the periphery of the face, typically over the upper third or quarter of the excavated profile (Figure 2) (35). Several researches have been conducted to assess the influence of the umbrella arch method on minimizing ground settlements regarding the ground-pipe interaction (11, 36-38). The reinforcement mechanism of UAM is to provide stability in both longitudinal and transverse directions of tunnel face through an arch-shaped support system. The term "steel-pipe-reinforced UAM" refers to the reinforcement mechanism in which the forepoles (steel pipes) are applied circumferentially through the tunnel face in the umbrella arch method. The reinforcement mechanism of this method is comprised of two critical phases: (1) structural reinforcement provided by pipes, and (2) the cement-shell formed by grouting improves the mechanical properties of the ground (39). According to Song et al. (40), the forepoles installed circumferentially through the tunnel face transfer the pressure of the earth to the primary support. In the longitudinal direction, the overall behavior of the pipes in terms of axial force, bending moment, and structural deformations are mechanically analogous to free-end beams with the other end engaged in the ground (41). Thus, in order to carry the earth pressure, one end of the UAM rests on the primary support system and, the other end is anchored to the ground in front of the tunnel face.

By carrying the earth pressure in this way, UAM provides the following advantages (42):

- Constraining settlements ahead of the tunnel face
- Increasing stability of the face
- Reducing the total cost of tunnel support
- Accelerating the excavation by enlarging the cutter face for machinery

Hence, as shown in Figure 3, the UAM technique adequately improves the stability of unsupported span prior to tunnel primary support installation (39).

2. DATA PREPARATION AND PRE-PROCESSING

The training and evaluation of MLP-ANN and SVR is carried out on a dataset from a series of centrifuge test reported by Le (18). The details of the centrifuge

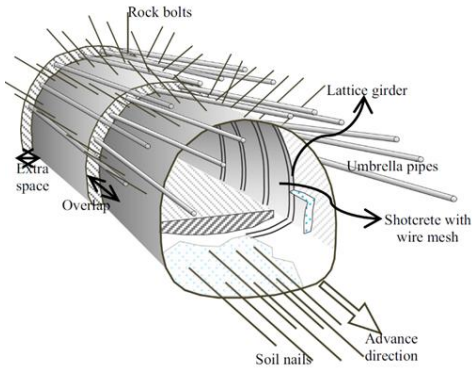

Figure 2. Schematic of umbrella arch implementation (35)

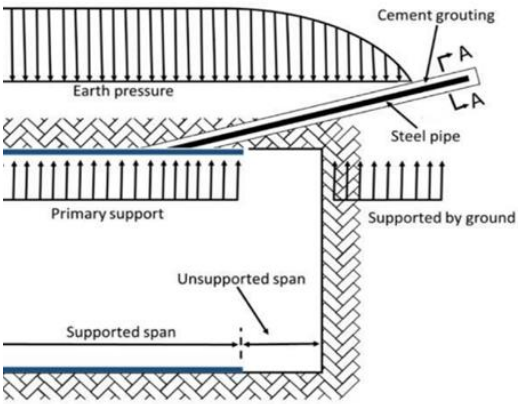

Figure 3. UAM ground reinforcement mechanism (40)

experiments can be found in Le (18) and briefly described below.

A typical model of a centrifuge experiment simulating a UAM, consisting of modelled pipes (forepoles), is depicted in Figure 4. The dimensions of the model are 550mm long, 200mm wide and the height of either 157mm or 257mm depending on the cover depth *C*. The models were tested at 125g. By the means of the advantageous capabilities of centrifuge modelling technique in replicating soil-structure interaction and the well-established scaling laws, at 125g the model represents a corresponding tunnel of 6.25m diameter at the depths of z_0 = 9.4m (for *C/D* = 1 cases) or z_0 = 22m (for *C/D*=3 cases). The experiments were conducted by gradually reducing the tunnel support pressure to simulate the tunnel excavation process. During the tests, important data such as tunnel support pressure, subsurface ground deformations and surface settlement were recorded for later analysis. The dataset considered in this paper comprises seven variables and the resulting maximum surface settlement (S_{max}). The variables cover the following:

- The forepoles characteristics: the spacing (U_{spacing}, L_{spacing}), the symmetric crown coverage angle of the forepoles (α), the pipe flexural rigidity (*EI*), the ratio of the forepole embedded length (*EL*) to tunnel diameter (*EL/D*),
- The tunnel face support pressure (P_s), and
- the ratio of cover depth to tunnel diameter (*C/D*).

A schematic description of the model parameters is demonstrated in Figure 5. Due to the limited nature of physical modeling, the experiments were conducted in specific scenarios (see Table 1). U_{spacing} and L_{spacing} are the spacing between crown (upper) and shoulder (lower) forepoles, respectively. The values of U_{spacing} and L_{spacing} were identical in the case of α=90º, due to the uniform distribution of pipes through tunnel periphery.

In the case of α=75º, the crown pipes were spatially concentrated compared to the shoulder pipes with 1.7 mm and 3.4 mm for crown and shoulders, respectively.

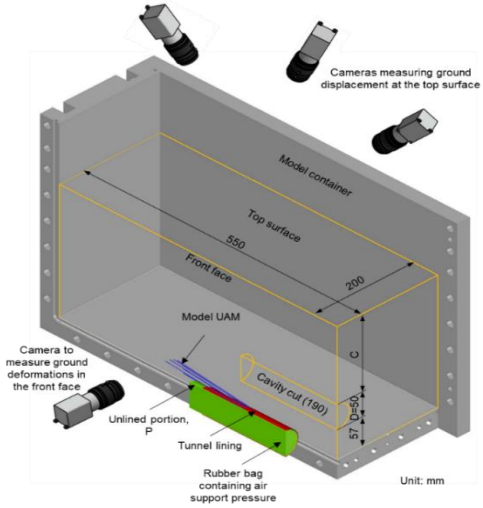

Figure 4. A typical model for centrifuge test (After (18))

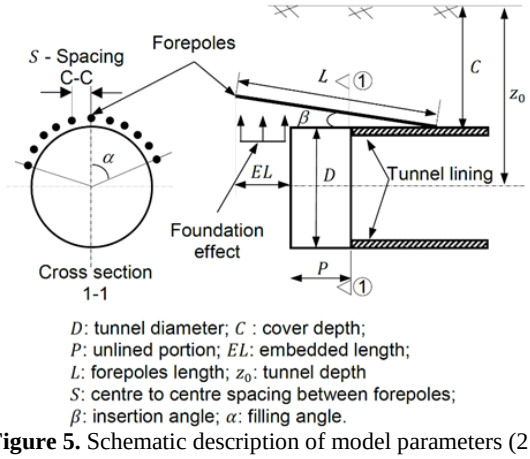

Figure 5. Schematic description of model parameters (21)

TABLE 1. Experimental configuration for adopted data (18)

Feature	Values	Comment
$U_{spacing}$	0, 1.7, 3	value depends on α
$L_{spacing}$	0, 3.4, 3	value depends on α
α	0, 75°, 90°	-
EI	0, 1.32, 2.52	zero indicates no forepoles were installed
EL/D	0, 0.5, 1	-
P_s	varied	pressure decreased from 175 kPa to 0 (to simulate face collapse)
C/D	1, 3	-
S_{max}	varied	-

In order to facilitate the extraction of meaningful insights from the dataset, the preprocessing procedure is necessary. For this purpose, the *MinMax* scaler of the Scikit library of Python package version 3.7 was used.

The aftermath of the above procedure is a high-resolution dataset, where the variation of each feature is in the range of [0, 1]. Upon normalization, the order of observations was shuffled to maintain the dynamicity of feature space while segregating the data into the train, test and, validation subsets.

Pearson's correlation coefficient is a covariance-based statistical measure to express the statistical relationship or association between two continuous variables. This procedure provides the magnitude of sensitivity (correlation) as well as its direction. Pearson's *R* method is generally utilized in linear regression. The basic formula of *R* for classic linear regression problems is given in the equation below (43).

$$R_{xy} = \frac{n\sum_{i=1}^{n} x_i.y_i - \left(\sum_{i=1}^{n} x_i\right).\left(\sum_{i=1}^{n} y_i\right)}{\sqrt{n.\sum_{i=1}^{n} x_i^2 - \left(\sum_{i=1}^{n} x_i\right)^2}.\sqrt{n.\sum_{i=1}^{n} y_i^2 - \left(\sum_{i=1}^{n} y_i\right)^2}} \quad (4)$$

where R_{xy} and n are Pearson's coefficients indicating the correlation between variables x and y and, number of observations, respectively. The calculated value for R_{xy} can range from +1 to -1.

3. AI ANALYSIS ON DATASET

3. 1. Artificial Neural Networks (ANNs) Artificial neural networks are intelligent dynamic systems based on experimental data that do not require any presumptions and transfer the knowledge or law behind the data to the network structure through processing on the train data. ANNs are amongst the most popular machine learning algorithms in geotechnics (28, 44, 45). A multilayer perceptron artificial neural network (MLP-ANN) was applied to analyze the nonlinear relationship between the aforementioned input variables and corresponding induced settlement. Initially, a subset comprising 439 observations of the normalized dataset was chosen to train the model, while the remnant 50 data were designated for validation. A sequential model with three dense layers was created in the Tensorflow-Keras library of Python version 3.7. The layers had 7, 12 and, 8 nodes, respectively. A schematic representation of the model network is shown in Figure 6. The activation functions of the two first layers were rectified linear unit (ReLU) and Sigmoid for the third layer. A 5-fold cross-validation technique was adopted to train the model in 150 epochs, with one-third of the data dedicated to testing the model performance at each iteration.

A stochastic gradient descendant (SGD) compiler with a momentum of 0.97 at 0.01 learning rate was utilized to specify the efficient weights. Mean-squared-error (*MSE*) and mean-absolute-error (*MAE*) metrics were employed to assess the total performance of the model while training. Also, the model loss was evaluated via *MSE* after each iteration.

3. 2. Support Vector Regression (SVR) Support vector regression is a type of support vector machine (SVM) that has been particularly developed for regression analysis. In SVR, efforts are taken to find a hyperplane (a line in two dimensions) and tune it in a manner that fits the data. The objective function of the SVR is to minimize the l_2-norm of the coefficient vector while subjecting it to a specific margin so-called epsilon-tube (46). In addition, for any values exceeding the thresholds of the epsilon-tube, a penalty (slack variable) is defined. The slack variable denotes the derivation of the penalized value from the closest margin. An extended form of the objective function of SVR is as follows (47):

$$MIN\ \frac{1}{2}\|w\|^2 + C\sum_{i=1}^{n}|\xi_i| \quad (5)$$

Subjected to:

$$|y_i - w_i x_i| \le \varepsilon + |\xi_i| \quad (6)$$

where w_i, C, ε_i, y_i, x_i and ε are the coefficient, regularization factor, slack variable, target value (label), input value (features) and epsilon-tube margin of the i-th observation, respectively. The SVR module of sklearn library of Python version 3.7 was used to conduct support vector regression analysis. A radial basis function (RBF) was adopted as a kernel to compile the support vector-driven model. The RBF kernel represents feature vectors in feature space. This feature vector (K) for a pair of two samples x_1 and x_2 is defined as follows (48):

$$K(x_1, x_2) = \exp\left(-\frac{\|x_1 - x_2\|^2}{2\sigma^2}\right) \quad (7)$$

where the term $\|x_1 - x_2\|^2$ is the squared Euclidean distance between x_1 and x_2, and σ is a free parameter. The values of 0.1 and 10 were configured to epsilon-tube margin (ε)

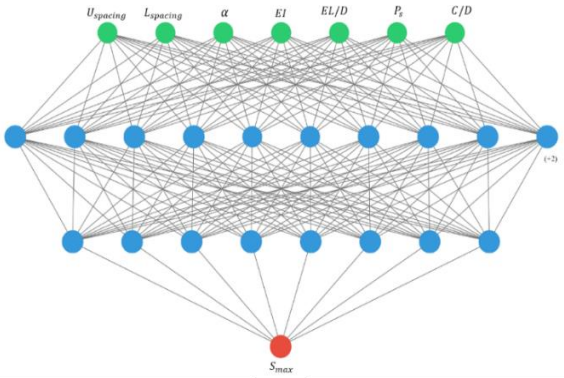

Figure 6. MLP-ANN network structure of the used model

and coefficient of regularization (*C*), respectively. Similar to ANN model, the SVR model was fitted for a subset comprising 439 observations of the normalized dataset and, the remnant 50 data were designated for validation.

4. MODEL PERFORMANCE EVALUATION

Mean-absolute-error (MAE), mean-squared-error (MSE), Nash-Sutcliffe (NSE), Kling-Gupta (KGE), and median-absolute-error (MedAE) were chosen to evaluate the efficiency of both models in training and testing process. MAE denotes the 1 norm fraction of all absolute error vectors per the total number of samples and is defined as follows (49):

$$MAE = \frac{\sum_{i=1}^{n}(x_i - \bar{x}_i)}{n} \quad (8)$$

where the term $(x_i - \bar{x}_i)$ refers to the absolute error vector between the observed x_i and predicted $\bar{x}_i$ values and n is the number of total samples. Similarly, the MSE indicates the mean of the squared absolute error vectors per the total number of samples within the dataset and is defined as follows (50):

$$MSE = \frac{\sum_{i=1}^{n}(x_i - \bar{x}_i)^2}{n} \quad (9)$$

NSE is the model goodness-of-fit evaluation index that has been proposed by Nash and Sutcliffe (51). NSE formula is expressed in Equation 10 (50).

$$NSE = 1 - \frac{\sum_{i=1}^{n}(\hat{Y}_i - Y_i)^2}{\sum_{i=1}^{n}(Y_i - \bar{Y})^2} \quad (10)$$

where $\hat{Y}_i$, Y_i and $\bar{Y}$ are predicted, observed, and mean of observed values, respectively. Since the NSE was unbiased, Gupta et al. (51) developed a novel criterion for model performance assessment that comprises a bias component. They proposed an improved version of the Nash-Sutcliffe efficiency index as follows (51).

$$KGE = 1 - ED \quad (11)$$

$$ED = \sqrt{(r-1)^2 + (\alpha-1)^2 + (\beta-1)^2} \quad (12)$$

where *ED*, *r*, α and β are the Euclidean distance from the ideal point; the linear correlation coefficient between observed and predicted values; the coefficient that describes relative variability within predicted and observed values; the ratio of mean predicted to mean observed values (bias), respectively.

The median-absolute-error is a loss criterion calculated by taking the median of all absolute differences between the predicted and observed values. One of the considerable advantages of MedAE is its robustness to outliers. MedAE is defined as the following (52):

$$MedAE(y, \hat{y}) = median(|y_1 - \hat{y}_1|, ..., |y_n - \hat{y}_n|) \quad (13)$$

5. RESULTS AND DISCUSSION

The experimental data of the geotechnical centrifuge of the City University of London were used to train and validate the predictive models (18). A statistical description of the normalized dataset for this study is given in Table 2. In addition, the histograms of normalized values are shown in Figure 7. The histograms depict the distribution of the values of each parameter on a normalized scale between 0 and 1. According to these histograms, the variation of *C*/*D* ratio, forepole spacing ($U_{Spacing}$, $L_{Spacing}$), *EL*/*D* ratio, α, and pipe *EI* were solely limited to 2, 3, 3, and 3 values, respectively. This was due to the limitations of the physical modeling of this study since the tests were conducted in certain scenarios (i.e., *C*/*D*=1, *C*/*D*=3, etc.). Pearson's correlation coefficient was employed to assess the parameter-wise sensitivity of features in this study. The correlation heatmap of the variables of this study is demonstrated in Figure 8. According to Figure 8, the P_s, *C*/*D* ratio, pipe *EI*, spacing of crown forepoles ($U_{spacing}$), α had the most significant correlation with maximum surface settlement while the spacing of shoulder forepoles ($L_{spacing}$) and *EL*/*D* ratio had relatively low correlation with the maximum surface settlement. Among all the input variables, solely the *C*/*D* ratio had a direct relationship with the maximum surface settlement. Also, the results indicate a considerable correlation between input variables which may be typically due to the test configuration of this study. For

TABLE 2. Statistical description of the normalized dataset

	$U_{spacing}$	$L_{spacing}$	α	Pipe *EI*	*EL/D*	P_s	*C/D*	S_{max}
count	489	489	489	489	489	489	489	489
mean	0.74	0.80	0.82	0.67	0.57	0.33	0.67	0.21
std	0.35	0.32	0.33	0.34	0.31	0.24	0.47	0.24
min	0.0	0.0	0.0	0.0	0.0	0.0	0.0	0.0
25%	0.57	0.88	0.83	0.52	0.5	0.15	0.0	0.035
50%	1.0	0.88	1.0	0.52	0.5	0.26	1.0	0.1
75%	1.0	1.0	1.0	1.0	1.0	0.48	1.0	0.33
Max	1.0	1.0	1.0	1.0	1.0	1.0	1.0	1.0

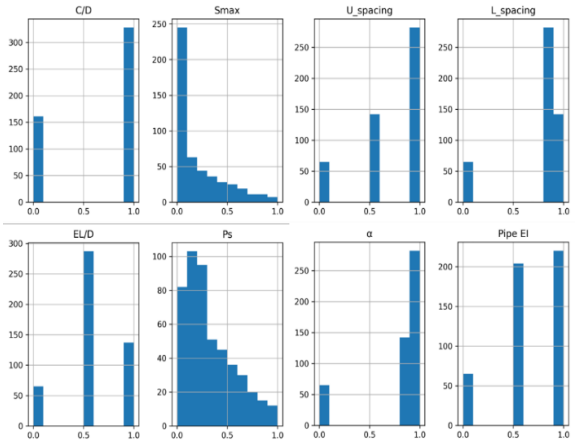

Figure 7. Histograms of normalized values

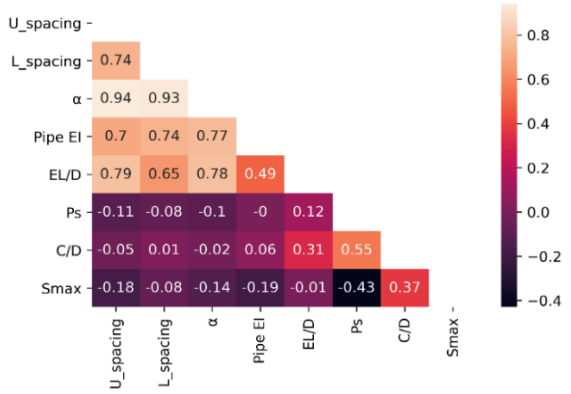

Figure 8. The heatmap of Pearson's correlation coefficients calculated for studied variables

instance, the *R* coefficient values of α addressing the correlation between the $U_{spacing}$ and $L_{spacing}$ were 0.94 and 0.92, respectively. In order to overcome these inconveniences, further investigations incorporating numerical finite element simulations are suggested.

5. 1. Artificial Neural Networks (ANNs) During the model training procedure, the score of each fold was specified as model loss and *MSE* criteria. The score-per-fold values are given in Table 3. The average scores for all folds were 0.035 and 0.003 for *MSE* and loss criterion, respectively. Diagram histories of the trained model accuracy and loss criterion are illustrated in Figure 9. Considering the model loss diagrams in train and test steps, it is apparent that the model yields ultimate convergence amid the implementation of the assumed network setup. The overall values of *MAE* and *MSE* were 0.026 and 0.001, respectively.

For the sake of comparison, a simple linear regression analysis was utilized to assess the correlation between

TABLE 3. Score-per-fold values for ANN model

Fold No.	Loss	*MSE*
1	0.0028	0.0354
2	0.0024	0.0334
3	0.0026	0.0352
4	0.0024	0.0345
5	0.0026	0.0353

predicted and observed values. The plot of linear regression analysis for the *ANN* predictory model is illustrated in Figure 10a. In addition, the predicted values for validation data are compared with the observed data in Figure 10b.

5. 2. Support Vector Regression (SVR) A similar validation configuration was evaluated for the *SVR* model. Since the specification of hyperplane geometry (tuning) conveys solely in one iteration, this process acts independently from iteration-based error analysis. Hence, unlike the MLP-ANN model, only the model's overall performance will be assessed in terms of *MAE* and *MSE*. The linear regression plot for *SVR* model is shown in Figure 11a. Additionally, Figure 11b illustrates a comparative analysis between observed and predicted values of maximum surface settlement. The *MAE* and *MSE* values for the trained model were 0.063 and 0.006, respectively. As represented in Figure 11b, the majority of validation data were inside the epsilon tube.

5. 3. Comparative Analysis for Trained Models The calculated NSE, KGE and, MedAE values for developed MLP-ANN and SVR models are summarized in Table 4. Respectively, the closer the NSE, KGE, and MedAE values are to 1, 1, and, 0, the more efficient the model performance. Therefore, according to Table 4, the MLP-ANN model is relatively more efficient than the SVR model in terms of NSE, KGE, and, MedAE. The aftermath of the comparative analysis indicates the superiority of the MLP-ANN model compared to the SVR model. The results of comparative analysis for both models were in alignment with the results of similar studies in terms of performance (28, 29, 31).

TABLE 4. Model performance evaluation for ANN and SVR

Criterion	Value	
	MLP-ANN	SVR
NSE	0.977	0.92
KGE	0.971	0.89
MedAE	0.0177	0.067

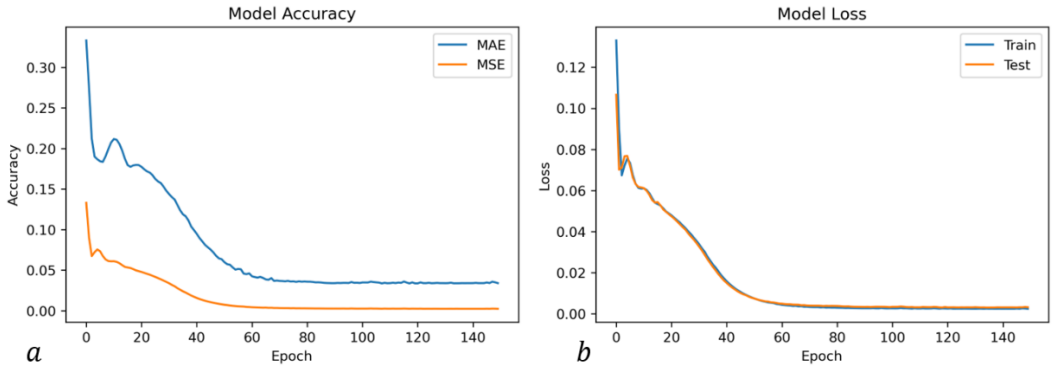

Figure 9. ANN-model performance evaluation diagrams: (a) Model training accuracy in terms of MAE and MSE; (b) Model loss for train/test data

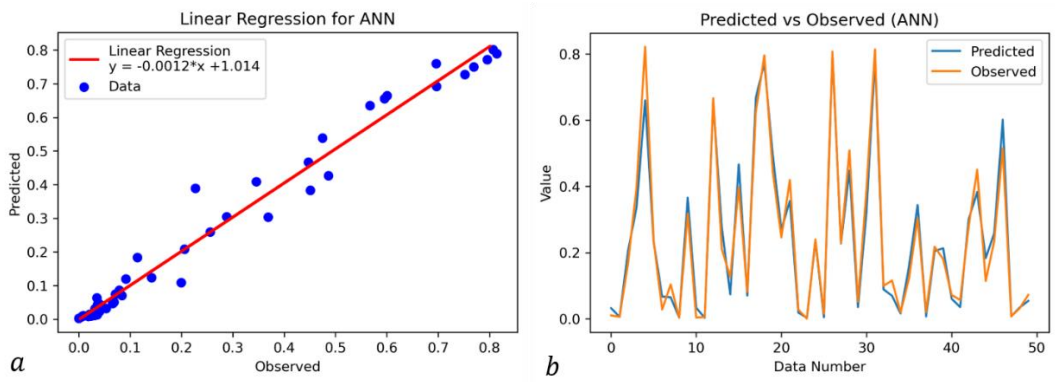

Figure 10. (a) Linear regression analysis and (b) comparison between MPL-ANN predicted and observed values for maximum surface settlement

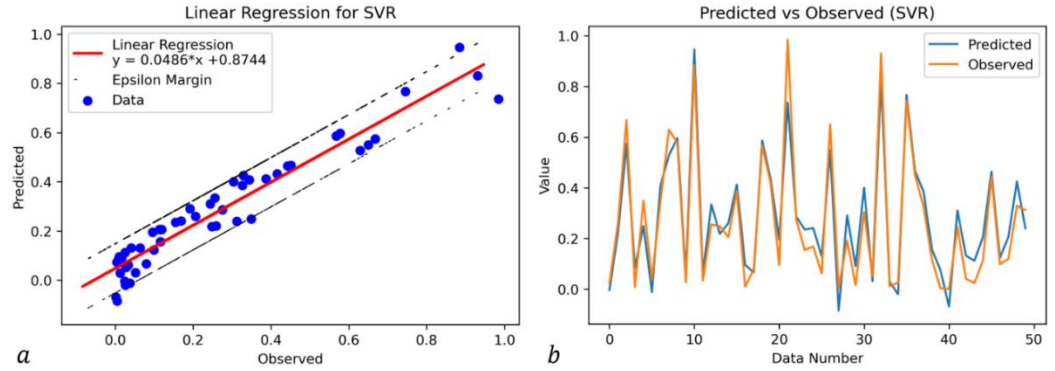

Figure 11. (a) Linear regression analysis and (b) comparison between MPL-ANN predicted and observed values for maximum surface settlement

6. CONCLUSIONS

Since the drastic tunneling-induced ground surface settlements can inevitably lead to catastrophic damage to adjacent structures, appropriately constraining the ground deformations to a tolerable extent is vital. For this purpose, a proper estimation of the settlement trough is required. The literature review of this study suggested that the empirical methods of settlement estimation fail to perform accurately and provide reliable outputs. Since the influence of UAM characteristics in developing the predictory models was not evaluated, a novel approach was suggested to predict the maximum ground surface settlement caused by tunneling, incorporating the characteristics of the umbrella arch method. In this context, the laboratory data were adopted from the City

University of London geotechnical centrifuge and utilized to train and validate MLP-ANN and SVR predictory models. The mechanical properties of the soil model were disregarded to provide a non-site-specific behavior to the trained models. The salient findings of this study are as follows.

The parametric sensitivity analysis indicates that the P_s, *C/D* ratio, pipe flexural rigidity (pipe *EI*), spacing of crown forepoles (U_{spacing}), and symmetric crown coverage angle (α) have the most significant correlation with the maximum ground surface settlement while the spacing of shoulder forepoles (L_{spacing}) and *EL/D* ratio have a relatively low correlation. Among all the input variables, solely the *C/D* ratio has a direct relationship with the S_{max}.

Both trained models yield promising results. Nevertheless, a negligible derivation was observed between the predicted values of the two models. The MLP-ANN model performed relatively more accurately than the SVR model. The aftermath of error analysis in terms of Nash-Sutcliffe efficiency, Kling-Gupta efficiency, and median-absolute-error was analogous for both models. The NSE, KGE, and MedAE indicate the relative superiority of MLP-ANN over SVR.

The yielded R^2 value of the regression analysis for SVR and MLP-ANN were 0.92 and 0.98, respectively. Thus, the MLP-ANN can be regarded as one of the adequate approaches for tunneling-induced settlement predictions.

With respect to the considerable correlation between UAM characteristics and the S_{max}, the suggested approach can be effectively used for estimating ground surface displacements where contextual mechanical properties are absent.

Although a significant correlation was observed between the implemented UAM characteristics and the corresponding maximum surface settlement, further researches comprising the supplementary numerical analysis are recommended on this subject, in order to cope with the limitations associated with the test configuration of this study.

7. ACKNOWLEDGMENTS

7. 1. Conflict of Interest Hereby, all authors acknowledge that they have no affiliations with or involvement in any organization or entity with any financial interest or non-financial interest in the subject matter or materials discussed in this manuscript. All authors read and approved the final manuscript.

7. 2. Data Availability Statement All data generated or analyzed during this study are available upon reasonable request.

7. 3. Funding Details The authors declare that no funds, grants, or other support were received during the preparation of this manuscript.

8. REFERENCES

1. Ocak I. Control of surface settlements with umbrella arch method in second stage excavations of Istanbul Metro. Tunnelling and Underground Space Technology. 2008;23(6):674-81. https://doi.org/10.1016/j.tust.2007.12.005
2. Yahya S, Abdullah R. A review on methods of predicting tunneling induced ground settlements. Electronic Journal of Geotechnical Engineering. 2014;19:5813-26.
3. Lee K, Rowe RK, Lo K. Subsidence owing to tunnelling. I. Estimating the gap parameter. Canadian geotechnical journal. 1992;29(6):929-40. https://doi.org/10.1139/t92-104
4. O'reilly MP, New B. Settlements above tunnels in the United Kingdom-their magnitude and prediction. 1982. Report No.: 090048862X.
5. Moussaei N, Khosravi MH, Hossaini MF. Physical modeling of tunnel induced displacement in sandy grounds. Tunnelling and Underground Space Technology. 2019;90:19-27. https://doi.org/10.1016/j.tust.2019.04.022
6. Alipenhani B, Bakhshandeh Amnieh H, Majdi A. Application of finite element method for simulation of rock mass caving processes in block caving method. International Journal of Engineering, Transactions A: Basics. 2023;36(1):139-51. https://doi.org/10.5829/IJE.2023.36.01a.16
7. Hashemi S, Naderi R. Application of random radial point interpolation method to foundations bearing capacity considering progressive failure. International Journal of Engineering, Transactions A: Basics. 2023;36(2):264-75. https://doi.org/10.5829/ije.2023.36.02b.07
8. Mashayekhi MA, Khanmohammadi M. Numerical Studies on Performance of Helical Pile-supported Embankments Over Soft Clay. International Journal of Engineering, Transactions A: Basics. 2024;37(4):596-607. 10.5829/IJE.2024.37.04A.03
9. Attewell PB, Yeates J, Selby AR. Soil movements induced by tunnelling and their effects on pipelines and structures. 1986. https://doi.org/10.1016/0886-7798(87)90195-7
10. Zhao C, Alimardani Lavasan A, Barciaga T, Schanz T. Mechanized tunneling induced ground movement and its dependency on the tunnel volume loss and soil properties. International Journal for Numerical and Analytical Methods in Geomechanics. 2019;43(4):781-800. https://doi.org/10.1002/nag.2890
11. Klotoé CH, Bourgeois E. Three dimensional finite element analysis of the influence of the umbrella arch on the settlements induced by shallow tunneling. Computers and Geotechnics. 2019;110:114-21. https://doi.org/10.1016/j.compgeo.2019.02.017
12. Boonsiri I, Takemura J. Observation of ground movement with existing pile groups due to tunneling in sand using centrifuge modelling. Geotechnical and Geological Engineering. 2015;33:621-40. https://doi.org/10.1007/s10706-015-9845-0
13. Khosravi MH, Takemura J, Pipatpongsa T, Amini M. In-flight excavation of slopes with potential failure planes. Journal of Geotechnical and Geoenvironmental Engineering. 2016;142(5):06016001. https://doi.org/10.1061/(ASCE)GT.1943-5606.0001439
14. Juneja A, Hegde A, Lee F, Yeo C. Centrifuge modelling of tunnel face reinforcement using forepoling. Tunnelling and

Underground Space Technology. 2010;25(4):377-81. https://doi.org/10.1016/j.tust.2010.01.013

15. Ertan T, Wu W, Erken A, Idinger G, editors. The Investigation of Stability of Tunnels and Settlements with Centrifuge Modeling2013: International Student Conference of Civil Engineering.
16. Divall S, Taylor RN, Xu M. Centrifuge modelling of tunnelling with forepoling. International Journal of Physical Modelling in Geotechnics. 2016;16(2):83-95. https://doi.org/10.1680/jphmg.15.00019
17. Ritter S, Giardina G, DeJong MJ, Mair RJ. Centrifuge modelling of tunneling-induced settlement damage to 3D-printed surface structures. 2016.
18. Le B. The effect of forepole reinforcement on tunnelling-induced movements in clay: City, University of London; 2017.
19. Le BT, Taylor RN. The reinforcing effects of Forepoling Umbrella System in soft soil tunnelling. Steel pipe. 2017;2000:70-80.
20. Le BT, Taylor R. Ground response to tunnelling incorporating soil reinforcement system. Canadian Geotechnical Journal. 2019;56(11):1719-28. https://doi.org/10.1139/cgj-2018-0075
21. Lu H, Shi J, Wang Y, Wang R. Centrifuge modeling of tunneling-induced ground surface settlement in sand. Underground Space. 2019;4(4):302-9. https://doi.org/10.1016/j.undsp.2019.03.007
22. Rahmanpour M, Osanloo M. Application of fuzzy linear programming for short-term planning and quality control in mine complexes. Journal of the Southern African Institute of Mining and Metallurgy. 2017;117(7):684-94. https://doi.org/10.17159/2411-9717/2017/V117N7A10
23. Sarfaraz H, Khosravi MH, Pipatpongsa T, Bakhshandeh Amnieh H. Application of artificial neural network for stability analysis of undercut slopes. International Journal of Mining and Geo-Engineering. 2021;55(1):1-6. https://doi.org/10.22059/IJMGE.2020.292606.594832
24. Rezaei M, Majdi A, Monjezi M. An intelligent approach to predict unconfined compressive strength of rock surrounding access tunnels in longwall coal mining. Neural Computing and Applications. 2014;24:233-41. https://doi.org/10.1007/S00521-012-1221-X/FIGURES/11
25. Majdi A, Beiki M. Applying evolutionary optimization algorithms for improving fuzzy C-mean clustering performance to predict the deformation modulus of rock mass. International Journal of Rock Mechanics and Mining Sciences. 2019;113:172-82. https://doi.org/10.1016/J.IJRMMS.2018.10.030
26. Asadizadeh M, Majdi A. Developing new Adaptive Neuro-Fuzzy Inference System models to predict granular soil groutability. International Journal of Mining and Geo-Engineering. 2019;53(2):133-42. https://doi.org/10.22059/IJMGE.2018.255209.594728
27. Shahrour I, Zhang W. Use of soft computing techniques for tunneling optimization of tunnel boring machines. Underground space. 2021;6(3):233-9. https://doi.org/10.1016/j.undsp.2019.12.001
28. Zhang L, Wu X, Ji W, AbouRizk SM. Intelligent approach to estimation of tunnel-induced ground settlement using wavelet packet and support vector machines. Journal of Computing in Civil Engineering. 2017;31(2):04016053. https://doi.org/10.1061/(asce)cp.1943-5487.0000621
29. Zhang P, Chen R-P, Wu H-N, Liu Y. Ground settlement induced by tunneling crossing interface of water-bearing mixed ground: A lesson from Changsha, China. Tunnelling and Underground Space Technology. 2020;96:103224. https://doi.org/10.1016/j.tust.2019.103224
30. Ahangari K, Moeinossadat SR, Behnia D. Estimation of tunnelling-induced settlement by modern intelligent methods. Soils and Foundations. 2015;55(4):737-48. https://doi.org/10.1016/j.sandf.2015.06.006
31. Bouayad D, Emeriault F, editors. Application of the hybrid ACP/ANFIS method for the prediction of surface settlement induced by an earth pressure tunnel boring machine with consideration of the encountered geology. Proceedings of the 8th European conference on numerical methods in geotechnical engineering, Delft, The Netherlands; 2014.
32. Moghaddasi MR, Noorian-Bidgoli M. ICA-ANN, ANN and multiple regression models for prediction of surface settlement caused by tunneling. Tunnelling and Underground Space Technology. 2018;79:197-209. https://doi.org/10.1016/j.tust.2018.04.016
33. Zhang K, Lyu H-M, Shen S-L, Zhou A, Yin Z-Y. Evolutionary hybrid neural network approach to predict shield tunneling-induced ground settlements. Tunnelling and Underground Space Technology. 2020;106:103594. https://doi.org/10.1016/j.tust.2020.103594
34. Hristova T, editor A model based on current harmonics for controlling the induction motor of a crusher. AIP Conference Proceedings; 2022: AIP Publishing.
35. Ocak I, Selcuk E. Comparison of NATM and umbrella arch method in terms of cost, completion time, and deformation. Arabian journal of geosciences. 2017;10(7):177. https://doi.org/10.1007/s12517-017-2938-8
36. Volkmann GM, Schubert W, editors. A load and load transfer model for pipe umbrella support. ISRM EUROCK; 2010: ISRM.
37. Volkmann G, Button E, Schubert W, editors. A contribution to the design of tunnels supported by a pipe roof. ARMA US Rock Mechanics/Geomechanics Symposium; 2006: ARMA.
38. Shi J, Zhang X, Chen L, Chen L. Numerical investigation of pipeline responses to tunneling-induced ground settlements in clay. Soil Mechanics and Foundation Engineering. 2017;54:303-9. https://doi.org/10.1007/s11204-017-9473-1
39. Morovatdar A, Palassi M, Ashtiani RS. Effect of pipe characteristics in umbrella arch method on controlling tunneling-induced settlements in soft grounds. Journal of Rock Mechanics and Geotechnical Engineering. 2020;12(5):984-1000. https://doi.org/10.1016/j.jrmge.2020.05.001
40. Song K-I, Cho G-C, Chang S-B, Lee I-M. Beam–spring structural analysis for the design of a tunnel pre-reinforcement support system. International journal of rock mechanics and mining sciences. 2013;59:139-50. https://doi.org/10.1016/j.ijrmms.2012.12.017
41. Bagherzadeh P, Goshtasbi K, Kashef M. Umbrella arch method performance, structural behavior and design elements utilizing in collapsing zones. Environmental Earth Sciences. 2020;79(23):521. https://doi.org/10.1007/s12665-020-09266-y
42. Muraki Y. The umbrella method in tunnelling: Massachusetts Institute of Technology; 1997.
43. Profillidis V, Botzoris G. Statistical methods for transport demand modeling. Modeling of transport demand. 2019:163-224. https://doi.org/10.1016/b978-0-12-811513-8.00005-4
44. Shahin MA, Maier HR, Jaksa MB. Predicting settlement of shallow foundations using neural networks. Journal of geotechnical and geoenvironmental engineering. 2002;128(9):785-93. https://doi.org/10.1061/(asce)1090-0241(2002)128:9(785)
45. Chen R, Zhang P, Wu H, Wang Z, Zhong Z. Prediction of shield tunneling-induced ground settlement using machine learning techniques. Frontiers of Structural and Civil Engineering. 2019;13(6):1363-78. https://doi.org/10.1007/s11709-019-0561-3
46. Smola AJ, Schölkopf B. A tutorial on support vector regression. Statistics and computing. 2004;14:199-222. https://doi.org/10.1023/B:STCO.0000035301.49549.88

47. Awad M, Khanna R, Awad M, Khanna R. Support vector regression. Efficient learning machines: Theories, concepts, and applications for engineers and system designers. 2015:67-80. https://doi.org/10.1007/978-1-4302-5990-9_4

48. Vert J-P, Tsuda K, Schölkopf B. A primer on kernel methods. 2004. https://doi.org/10.7551/mitpress/4057.003.0004

49. Everitt BS, Skrondal A. The Cambridge dictionary of statistics. 2010. https://doi.org/10.1017/cbo9780511779633

50. McCuen RH, Knight Z, Cutter AG. Evaluation of the Nash–Sutcliffe efficiency index. Journal of hydrologic engineering. 2006;11(6):597-602. https://doi.org/10.1061/(asce)1084-0699(2006)11:6(597)

51. Gupta HV, Kling H, Yilmaz KK, Martinez GF. Decomposition of the mean squared error and NSE performance criteria: Implications for improving hydrological modelling. Journal of hydrology. 2009;377(1-2):80-91. https://doi.org/10.1016/J.JHYDROL.2009.08.003

52. Bonnin R. Machine Learning for Developers: Uplift your regular applications with the power of statistics, analytics, and machine learning: Packt Publishing Ltd; 2017.

Persian Abstract

چکیده

پیش بینی دقیق نشست زمین برای جلوگیری از آسیب های شدید ساختاری و زیرساختی امری ضروری است. این مقاله به بررسی پیش بینی نشست زمین ناشی از تونل سازی با استفاده از مدل های یادگیری ماشین می پردازد. روش های تجربی پیش بینی نشست زمین اغلب غیر دقیق و موقعیت محور هستند. در این راستا، توسعه روش های جدید و دقیق پیش بینی برای جلوگیری از آسیب های فاجعه بار حیاتی است. روش نگهداری قوس چتری تغییر شکل های زمین را به منظور ایجاد پایداری اولیه قبل از اجرای سیستم نگهداری اصلی محدود می کند. در این مقاله مدل های یادگیری ماشین برای پیش بینی نشست زمین صرفا از طریق پارامترهای سیستم قوس چتری و بدون در نظر گرفتن ویژگی های خاک توسعه داده شده اند. بدین منظور از شبکه های عصبی مصنوعی پرسپترون چند لایه (MLP-ANN) و رگرسیون بردار پشتیبان (SVR) استفاده شده است. نتایج نشان می دهند که یادگیری ماشین بهتر از روش های تجربی عمل می کند. مدل مبتنی بر MLP-ANN از مدل مبتنی بر SVR با R^2 به ترتیب ۰.۹۸ و ۰.۹۲ برتری دارد. همچنین همبستگی قوی بین طراحی سیستم قوس چتری و نشست حاصله در سطح زمین مشاهده شد. روش پیشنهادی می تواند در شرایط در دسترس نبودن مشخصات مکانیکی محیط میزان نشست را به طور موثری پیش‌بینی نماید. به طور کلی، این مطالعه از یادگیری ماشین، به ویژه الگوریتم MLP-ANN، به عنوان یک جایگزین کارآمد و قابل اعتماد برای روش های تجربی برای پیش بینی نشست زمین ناشی از تونل سازی از طریق پارامترهای طراحی قوس چتری حمایت می کند.